Archives of Biochemistry and Biophysics 565 (2015) 68–75

Contents lists available at ScienceDirect

Archives of Biochemistry and Biophysics

journal homepage: www.elsevier.com/locate/yabbi

Nitric oxide enhances extracellular ATP induced Ca^{2+} oscillation in HeLa cells

Yinglong Tang [a,d,1], Yin Yin [b,1], Lin Miao [a], Bin Wei [c], Kui Zhai [a], Guangju Ji [a,*]

[a] National Laboratory of Biomacromolecules, Institute of Biophysics, Chinese Academy of Sciences, Beijing, China
[b] General Hospital of Air Force, Stomatology, Beijing, China
[c] Department of Physiology, Wayne State University School of Medicine, Detroit, MI 48201, United States
[d] University of the Chinese Academy of Sciences, Beijing 100049, China

ARTICLE INFO

Article history:
Received 8 August 2014
and in revised form 11 November 2014
Available online 25 November 2014

Keywords:
Nitric oxide
Calcium oscillation
eNOS
Phospholamban

ABSTRACT

Calcium (Ca^{2+}) oscillations play a central role in varieties of cellular processes including fertilization and immune response, but controversy over the regulation mechanisms still exists. It has been known that nitric oxide (NO) dependently regulates Ca^{2+} signaling in most physiopathological processes. Previous study indicated that eNOS translocation during some pathological process influences intracellular Ca^{2+} homeostasis. In this study, we investigated the role and mechanism of NO on Ca^{2+} release by overexpressing eNOS in cytoplasm (Cyto-eNOS) and endoplasmic reticulum (ER-eNOS) of HeLa cells. We found that the properties of Ca^{2+} release were altered by the overexpression of eNOS. The amplitude and frequency of extracellular ATP (eATP)-induced Ca^{2+} oscillation were enhanced in both Cyto-eNOS and ER-eNOS cells, respectively. Especially, the enhancement of the amplitude and frequency of the Ca^{2+} oscillation was much more significant in the ER-eNOS cells than that of Cyto-eNOS cells. Further study indicated that this effect was abrogated by NO inhibitor, L-NAME, suggesting it was not an artificial result induced by ER stress. Furthermore, an up-regulated phosphorylation of phospholamban (PLB) was observed and the sarco-endoplasmic reticulum Ca^{2+}-ATPase (SERCA) function was activated followed by the significant increase in the ER Ca^{2+} load. Taken together, we revealed a novel regulatory mechanism of Ca^{2+} oscillation.

Introduction

Calcium (Ca^{2+})[2] signaling mediates numerous cellular responses, including neurotransmitter release, muscle contraction, mitochondrial metabolism, gene expression and cell death and proliferation in nearly all eukaryotic cells. Among the different types of Ca^{2+} signals such as Ca^{2+} spark, Ca^{2+} transient and Ca^{2+} wave, Ca^{2+} oscillation is a special modulator with signaling information encoded in both amplitude and frequency [1,2]. Intracellular Ca^{2+} oscillations represent a universal signaling mode since they are observed in different types of cells [3]. Many events such as fertilization and immune response are activated by Ca^{2+} oscillations [4,5]. Researchers have observed a kaleidoscope of Ca^{2+} oscillations but perhaps most interest has been kindled by the finding that cytosolic Ca^{2+} ($[Ca^{2+}]c$) oscillates repetitively in response to low doses of agonist [1]. ATP, an extracellular physiological signal molecule which regulates many cellular processes including secretion and transcription [6,7], induces Ca^{2+} oscillations by activating phospholipase C (PLC)-associated P2Y purinergic receptors, leading to production of inositol 1,4,5-trisphosphate (IP3) and subsequent Ca^{2+} release (IICR) from intracellular stores in HeLa cells [8]. The regulation of eATP induced Ca^{2+} oscillation and the relationship to cell function is poorly understood.

Nitric oxide (NO), synthesized by the enzyme NO synthase (NOS), is a major factor in cardiovascular system by manipulating Ca^{2+} mobilization [9]. There are three main isoforms of the enzymes, named neuronal NOS (nNOS), inducible NOS (iNOS) and endothelial NOS (eNOS), of which eNOS can be activated by

* Corresponding author at: Institute of Biophysics, Chinese Academy of Sciences, Beijing Datun Rd. 15, Beijing 100101, China.
E-mail address: gj28@ibp.ac.cn (G. Ji).

[1] These authors contributed equally to this work.

[2] *Abbreviations used:* Ca^{2+}, calcium; NO, nitric oxide; Cyto-eNOS, eNOS in cytoplasm; ER-eNOS, eNOS in endoplasmic reticulum; eATP, extracellular ATP; PLB, phospholamban; SERCA, sarco-endoplasmic reticulum Ca^{2+}-ATPase; $[Ca^{2+}]c$, cytosolic Ca^{2+}; PLc, phospholipase C; IP3, inositol 1,4,5-trisphosphate; NOs, NO synthase; nNOS, neuronal NOS; iNOS, inducible NOS; eNOS, endothelial NOS; TBST, Tris-buffered saline-Tween 20; ECL, enhanced chemiluminescence; ISO, isoproterenol; L-NAME, hydrochloride; 2-APB, 2-aminoethoxydiphenyl borate; TG, thapsigargin; RYRs, ryanodine receptors.

http://dx.doi.org/10.1016/j.abb.2014.11.006
0003-9861/

receptor-dependent and -independent agonists as a consequence of an increase in the intracellular free Ca^{2+} concentration and the association of Ca/calmodulin complex with eNOS [10]. Besides activating by Akt-dependent phosphorylation at Ser1177 [11], it has been reported that eNOS can also be activated by translocation [12]. In some pathological process, like heart failure, eNOS disassociated with caveolin-3 in the sarcolemma, which suggests there is an increase of eNOS in the cytosol [13]. However, how this spatial change of eNOS influences Ca^{2+} homeostasis is still unknown.

In the present study, by overexpressing two differentially-located eNOS in HeLa cells, we have investigated the role and mechanism of eNOS in regulating eATP induced Ca^{2+} oscillation. We demonstrated that eNOS enhanced the oscillatory Ca^{2+} signals both in frequency and amplitude through phosphorylation of PLB. With the activation of SERCA by phosphorylated PLB, Ca^{2+} re-uptake efficiency and ER Ca^{2+} load were increased followed by the enhancement of the oscillation. Thus, we proposed a novel regulation mechanism to explain eATP induced Ca^{2+} oscillation in HeLa cells.

Materials and methods

Gene construction

eNOS gene fragments were amplified with the Hind III and EcoR I sites containing primers by using plasmid PM831221 containing the eNOS cDNA (provided by Marsden lab, GENE BANK NO. M95296) as the template. The restricted PCR fragments were ligated to the 5′ end of DsRed2 in pCMV (pEGFP-C2 without EGFP gene) to yield the plasmid for expressing eNOS and DsRed fusion proteins in mammalian cells.

ER-eNOS and ER-Red gene fragments were obtained by extending the eNOS cDNA at 5′ end with the endoplasmic reticulum (ER) targeting sequence of calreticulin and DsRed cDNA at 3′ end with the ER retention sequence (KDEL), respectively. ER-eNOS and ER-Red fusion gene fragments were cloned into pCMV to yield the eNOS and DsRed fusion proteins targeted to the mammalian cell's ER.

Cell culture and cell transfection

HeLa cell lines were cultured in H-DMEM medium supplemented with 10% fetal bovine serum, 100 μg/ml penicillin, and 100 μg/ml streptomycin. Cell transfection was executed following Lipofectamine 2000 protocols (Invitrogen, USA). Forty-eight hours after transfection, cells were collected for the maximum expression of target protein.

Western blot analysis

Western blotting was performed as previously described [14,15]. Briefly, to determine the expression level of the associated proteins in the transfected cells, cell lysate was collected 48 h after the transfection by using the RIPA lysis buffer containing 50 mM Tris (pH 7.4), 150 mM sodium chloride, 1% Triton X-100, 1% sodium deoxycholate, 0.1% SDS. The homogenates were centrifuged in a microcentrifuge at top speed for 5 min to remove insoluble materials, and protein concentration of the lysates were determined by BCA Protein Assay Kit (Beyotime), and then prepared using loading buffer containing 2% SDS and 1% β-mercaptoethanol, pH 8.8. The tissue homogenates were heated at 85 °C for 3 min, centrifuged in a microcentrifuge at top speed for 1 min every time before using. Immediately after heating about 30 μg of protein extracts were loaded onto a 12% acrylamide SDS–PAGE gel. The resolved proteins were transferred to PVDF membranes (Millipore) at 300 mA for 60 min (for the detection of phosphorylated proteins, NaF, Na_2VO_4 was added in the following buffers to inhibit the phosphatases). The membranes were blocked for 1 h with Tris-buffered saline-Tween 20 (TBST) containing 1% BSA at room temperature. The blocked membranes were immunoblotted with specific antibodies. After washing 5 times in TBST, the membranes were incubated in TBST containing 1% BSA and the secondary antibody conjugated to horseradish peroxidase. Final detection was performed using enhanced chemiluminescence detection solution 1 and 2 (1:1) (ECL; Millipore). GAPDH (Sigma) protein was detected as a control housekeeping protein to ensure equal protein loading in all experiments.

Confocal microscopy and calcium measurement

Transfected HeLa cells were cultured on coverslips for 2 days and then loaded with Ca^{2+}-sensitive dye fluo-4 AM (2 μM) (Molecular Probes, Eugene, OR, USA) in a standard solution containing (in mM) 140 NaCl, 5.5 KCl, 2 $CaCl_2$, 1 $MgCl_2$, 10 HEPES, 3 glucose, pH 7.4 at room temperature for 5–10 min. The cells were firstly excited at 543 nm to detect the DsRed expression. Then the excitation wavelength was changed to 488 nm to detect Ca^{2+} activity of the DsRed positive cells. To inhibit eNOS and IP_3R, cells were pretreated with 100 μM L-NAME and 10 μM 2-APB in the standard solution at room temperature before each experiment. To inhibit NCX, Na^+ was substituted with 140 mM N-methyl-glucosamine in the solution. To evaluate the effect of isoproterenol (ISO), HeLa cells were pretreated with 10 and 50 nM isoproterenol and then followed by a stimulation of 10 μM ATP in standard solution. For calcium store measurement, HeLa cells were perfused with 100 μM ATP plus 2 μM TG in 0-Ca^{2+} solution containing 5 mM EGTA. Ca^{2+} was measured by using a laser scanning confocal microscope (SP5, Leica), which was connected to Leica DMI6000 inverted microscope, using a Plan Apo ×40 oil objective (1.25 numerical aperture). A sequential scanning acquisition technique was used in order to avoid crosstalk. Images were collected every 573 ms for 2 min in a format of 512 × 512, 400 Hz scanning and the serial images were analyzed with Image J. Under our experimental conditions, fluorescent bleaching was not significant and. The Ca^{2+}-dependent fluorescence intensity ratio ($\Delta F/F0$) was plotted as a function of time. The mean baseline fluorescence intensity ($F0$) was obtained by averaging fluorescence value of the continuous 20 images without Ca^{2+} transient activity before application of ATP and the frequency of Ca^{2+} oscillation was calculated as total peak numbers during the stimulation.

NO measurement

Intracellular NO was measured with 3-amino,4-aminomethyl-2′,7′-difluorescein, diacetate (DAF-FM DA), as previously described [16]. Briefly, after HeLa cells were transfected with eNOS plasmids for 48 h, the cells were washed three times with PBS and then incubated in 5 μM DAF-FM DA at 37 °C for 20 min. After a further three PBS washes, the fluorescence was analyzed by Leica SP5 confocal microscope with excitation at 495 nm and emission at 515 nm within 15 min.

Chemicals and reagents

N^G-nitro-L-arginine methyl ester, hydrochloride (L-NAME) and DAF-FM DA was from Beyotime, Fluo-4 was from Molecular Probe, and 2-aminoethoxydiphenyl borate (2-APB) was from Calbiochem. IP_3R1 antibody (sc-28614) was from Santa Cruz Biotechnology, SERCA2 antibody (MA3-919) was from Thermo Scientific, eNOS antibody (Cat: 610296) was from BD Biosciences; IP_3R3 (ab78556), PLB (ab2865) and p-PLB (Ser16) (ab15000) antibodies

were from Abcam. N-methyl-D-glucamine, thapsigargin (TG) and other chemicals were from Sigma.

Statistical analysis

Statistical analysis was performed by using Origin 8. Values given are means ± SEM. Data were tested for significance using the Student's *t*-test. Only results with P values <0.05 were considered statistically significant.

Results

eNOS overexpression enhances eATP induced calcium oscillation

eNOS translocation during some pathological processes has been observed [17,18]. However, the influence of this process on Ca^{2+} signaling is not clear. In the present study, we have constructed two eNOS overexpression plasmids with DsRed tag in cytoplasm (Cyto-eNOS) and endoplasmic reticulum (ER-eNOS) (Fig. 1A), respectively. 48 h after transfecting these plasmids into HeLa cell lines, we could easily distinguish the eNOS overexpressing cells from the others by confocal imaging (Fig. 1B). We observed that eNOS was expressed as a network level similar to the ER morphology (shown in the ER-eGFP) in the ER-eNOS cells (Fig. 1C). Comparably, eNOS was distributed evenly in the Cyto-eNOS cells. The formation of nitric oxide was observed by NO sensitive indicator 3-amino, 4-aminomethyl-2′,7′-difluorescein, diacetate (DAF-FM DA) in eNOS overexpressed cells (Fig. 1B). Moreover, Western blot analysis also confirmed that eNOS was overexpressed in the transfection cells and the expression levels of eNOS were not different between Cyto-eNOS and ER-eNOS cells. However, the control HeLa cells showed no eNOS expression, thus the endogenous interference could be excluded (Fig. 1D and E).

Confocal microscopy imaging study indicated that there was no spontaneous change of cytosolic Ca^{2+} levels in eNOS overexpressing cells or control cells. However, when the cells were exposed to 10 μM ATP, striking Ca^{2+} oscillations were observed both in Cyto-eNOS and ER-eNOS overexpressing cells (Fig. 2A); although only a small percentage of the control cells exhibited Ca^{2+} oscillation (Fig. 2B). As shown in Fig. 2C, the peak amplitude of Ca^{2+} oscillation ($\Delta F/F0$) in DsRed, Cyto-eNOS, ER-Red and ER-eNOS transfected cells was 1.22 ± 0.06, 4.41 ± 0.23, 1.28 ± 0.14, 5.01 ± 0.17, respectively. Compared to the controls, the peak amplitude of Ca^{2+} oscillation was increased by 2.61 and 2.91-fold in the Cyto-eNOS and ER-eNOS cells, respectively. Furthermore, we also found that the peak amplitude of Ca^{2+} oscillation of ER-eNOS cells was significantly higher than that of the Cyto-eNOS cells. Next, we explored the role of eNOS in the frequency modulation of Ca^{2+} oscillation. The duration of Ca^{2+} oscillation was about 90 s among all the cells detected, the numbers of spikes were used to indicate the frequency. As shown in Fig. 2E, the frequency of Ca^{2+} oscillation was also increased in the two types of eNOS transfected cells compared to the controls, and it was significant higher in ER-eNOS cells than that of Cyto-eNOS cells. We also used another IP3 agonist, histamine, to determine the effect of NO on calcium oscillation, and subsequently strong enhancements of amplitude and frequency were observed (Fig. S1). To ensure that this phenomenon was not the effect of ER stress caused by overexpressing eNOS, L-NAME, an inhibitor of eNOS, was used to inhibit the production of NO. As shown in Fig. 2D and F, in the presence of L-NAME both the eATP induced peak amplitude and frequency of Ca^{2+} oscillation were significantly reduced in the Cyto- and ER-eNOS cells.

Taken together, these results suggest that NO enhances the eATP induced Ca^{2+} oscillation both in the frequency and the amplitude, and the enhancement effect is more significant in ER-eNOS overexpressing cells.

eNOS regulates Ca^{2+} oscillation via phosphorylation of phospholamban

The finding that eNOS overexpression leading to the enhancement of Ca^{2+} oscillation encouraged us to investigate the mechanism further. As described above, ER-eNOS cells exhibited more significant Ca^{2+} oscillation than that of Cyto-eNOS, which suggested that NO influence the function of the ER Ca^{2+} pump. Indeed, as shown in Fig. 3A, PLB, a regulator of SERCA2, was highly phosphorylated by the overexpression of eNOS (Fig. 3A). Furthermore, the phosphorylation of PLB on serine 16 was much higher in the ER-eNOS overexpressing cells than that in the Cyto-eNOS cells (Fig. 3A), suggesting that disassociation of PLB from SERCA activated the Ca^{2+} recycling system during eATP stimulation process, resulting in high peak amplitude and frequency of Ca^{2+} oscillation. It is thought that cyclic-AMP-dependent phosphorylation of PLB is also an important regulatory mechanism of SERCA [19,20]. Therefore, we tested the effects of isoproterenol on eATP induced Ca^{2+} oscillation. As shown in the Fig. 3D and E, the amplitude ($\Delta F/F0$) of calcium oscillation was dramatically increased from 1.95 ± 0.06 to 4.56 ± 0.30-fold in DsRed overexpressed cells when incubated with 10 nM ISO, and the frequency was also increased from 1.90 ± 0.06 to 2.59 ± 0.20. Moreover, the effects of 50 nM ISO on calcium oscillation was much more significant than 10 nM. Similar results were also obtained in ER-Red overexpressed cells (Fig. 3D and E). Taken together, these results indicate that dose-dependent phosphorylation of PLB is associated with the enhanced calcium oscillation. It has been thought that NCX is also an important Ca^{2+} extruder [21] and therefore we next explored the role of NCX in modulation of Ca^{2+} oscillation. After inhibition of NCX by replacing Na^{2+} with 140 mM NMDG in extracellular solution [8], there was no significant alteration of Ca^{2+} oscillation observed in the eNOS expressed cells (Fig. 3F), suggesting that NCX was not involved in the regulation of Ca^{2+} oscillation mediated by NO.

Increased ER Ca^{2+} load is responsible for the higher amplitude of Ca^{2+} oscillation

The alteration of Ca^{2+} release properties induced by eNOS overexpression might also be due to either increase in IP_3R activity or the content of Ca^{2+} store, or both. When incubating the cells with 2-APB, 10 μM eATP induced-Ca^{2+} oscillation was entirely diminished, suggesting that intracellular calcium release through IP_3R was involved (Fig. 3C). Therefore, we next examined the expression levels of IP_3Rs and SERCA2. As shown in Fig. 3B, the expression levels of all the proteins determined were not significantly changed in the eNOS overexpressed cells, which suggested that the alteration of Ca^{2+} release properties induced by eNOS overexpression did not involve changes in the expression levels of either IP_3Rs or SERCA2. Then, what leads to the alteration of Ca^{2+} release properties in eNOS overexpressing cells? Previous studies suggested that the regulation of SERCA alters ER Ca^{2+} load [22]. Thus, we wondered whether the over-activation of SERCA could also achieve this effect. In the presence of 2 μM thapsigargin (TG), an inhibitor of SERCA, the cells were stimulated by 100 μM ATP to make sure the complete depletion of Ca^{2+} store. ER Ca^{2+} load was calculated as the integration of the normalized fluorescence value to time (Fig. 4A). As shown in Fig. 4B and C, compared to the control cells, the ER Ca^{2+} load was significantly increased in both Cyto-eNOS and

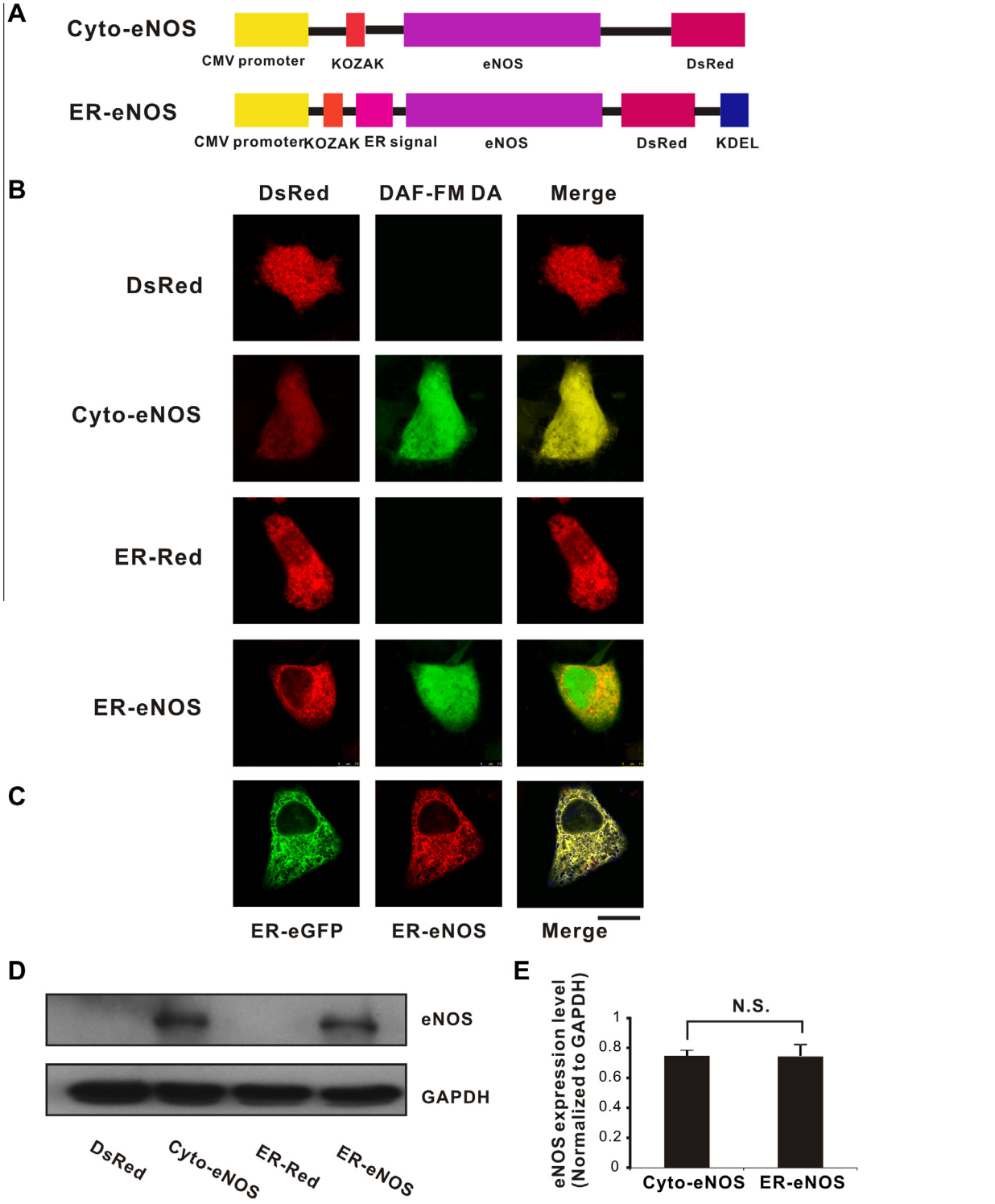

Fig. 1. Overexpression of eNOS in HeLa cells. (A) Plasmid construction of Cyto-eNOS and ER-eNOS for expression in HeLa cells. KOZAK: KOZAK consensus sequence, GCCACC; ER signal, ER targeting sequence of calreticulin; KD EL: ER retention sequence of KDEL. (B) Confocal images of HeLa cells expressed Cyto-eNOS and ER-eNOS (left panel) and the detection of NO by DAF-FM DA (middle panel) (scale bar = 15 μm as shown in C). (C) Cells transfected with ER-eNOS and ER-eGFP (scale bar = 15 μm). (D) Western blot analysis of eNOS expression in HeLa cells transfected with Cyto-eNOS and ER-eNOS plasmids. (E) Relative densitometric values of eNOS were analyzed by normalizing to GAPDH, no significant change was observed between Cyto and ER-eNOS overexpressing cells.

ER-eNOS cells; further analysis indicated that the ER Ca^{2+} load was much higher in the ER-eNOS cells than that in the Cyto-eNOS cells (Fig. 4D).

Taken together, these results suggest that the alteration of Ca^{2+} release properties induced by eNOS overexpression in HeLa cells is due to the increase in the ER Ca^{2+} load.

Discussion

The expression and activity of eNOS are changed in many pathological processes. It has been reported that educed eNOS activity and expression are involved in the onset of myocardial hypertrophy and increased cytokine expression, which finally leads to heart

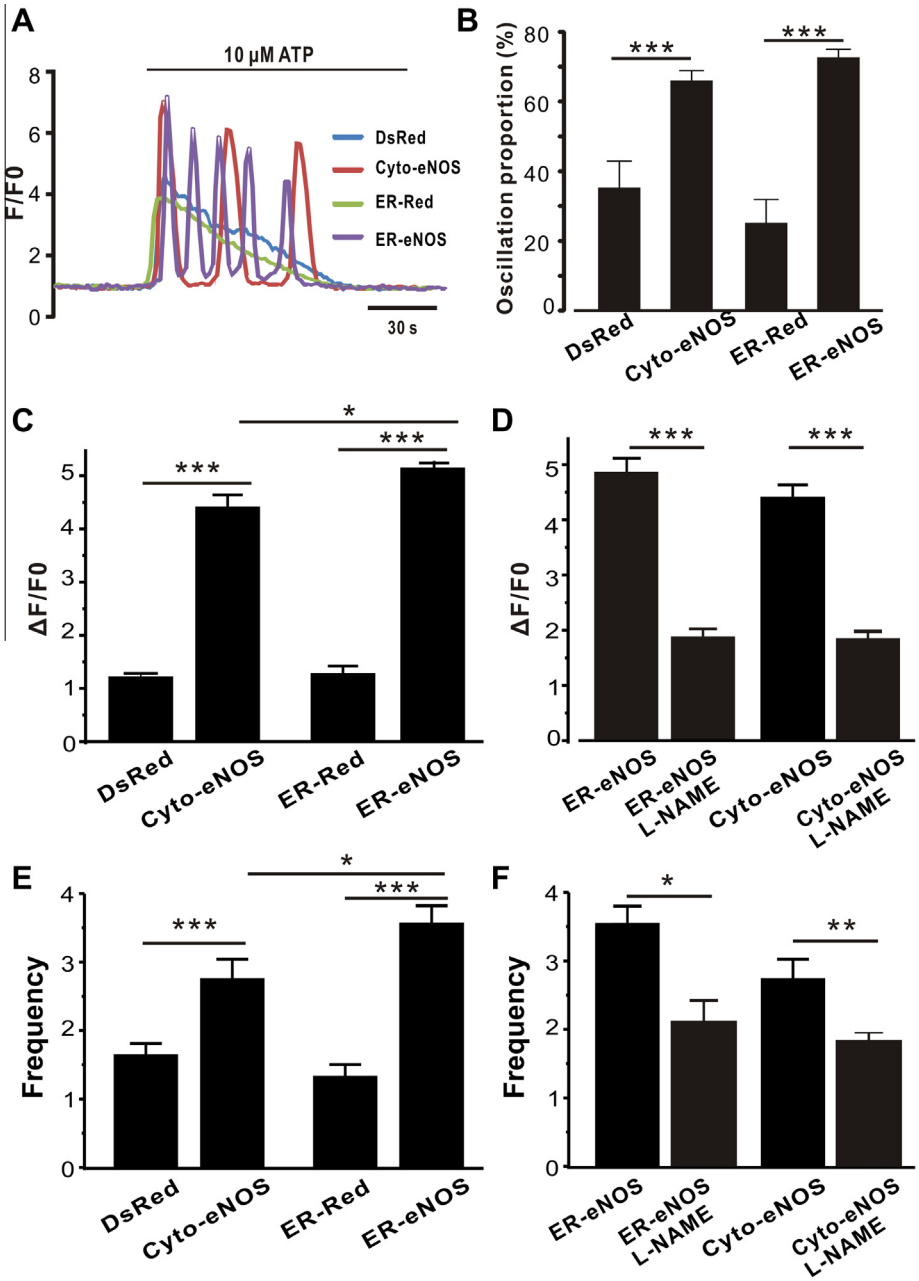

Fig. 2. eATP induced calcium oscillations in eNOS overexpressing cells. (A) Effects of extracellular ATP on $[Ca^{2+}]_C$ in HeLa cells transfected with DsRed, Cyto-eNOS, ER-Red and ER-eNOS; traces in the column arise from individual cell recordings. (B) Statistical results of Ca^{2+} oscillation proportion during ATP stimuli in the eNOS overexpressing cells and the control cells. (C) Summary data of eATP induced peak amplitude of Ca^{2+} transients in HeLa cells transfected by eNOS plasmids (n = 50–90 from 5 independent experiments). (D) Effects of L-NAME on the amplitude of Ca^{2+} transients in Cyto- and ER-eNOS expressed cells (n = 30 from 4 independent experiments). (E) Summary data of frequency of Ca^{2+} oscillation in the Cyto-eNOS and ER-eNOS overexpressing cells. (F) Effects of L-NAME on the frequency of Ca^{2+} oscillations in the Cyto- and ER-eNOS overexpressing cells. $^{*}P < 0.05$, $^{**}P < 0.01$ and $^{***}P < 0.0001$ by two-tailed Student's test.

failure [23]. Yet in the inflammatory responses there is a great increase in the eNOS activity which is mediated by the dissociation of eNOS from caveolin-1 [24]. However, whether this change influences Ca^{2+} signaling is still confused. In the present study, we have overexpressed eNOS in ER and cytosol, respectively, to explore the crosstalk between Ca^{2+} and NO. We did not find any Ca^{2+} activity in the basal level. However, 10 μM ATP induced Ca^{2+} oscillation was dramatically augmented in the eNOS overexpressing cells (Fig. 2). Previous studies had shown that ER stress causes the disturbance of Ca^{2+} signaling [25]; whereas, we found that the alteration of Ca^{2+} release properties induced by eNOS overexpression was significantly attenuated by L-NAME, suggesting that eNOS-derived NO contributed to the enhanced function of the extracellular physiological signal, like ATP. Through modulating Ca^{2+} signal the eNOS-derived NO may exert critical influences on the pathological process development.

Like electrical signals, the conventional view about the information carried by Ca^{2+} oscillation is encrypted in either the amplitude or frequency. The amplitude modulation is conceptually straightforward because it is governed by Ca^{2+} affinity of the sensor or decoder. However, in the frequency modulation, the downstream Ca^{2+} sensor, like PKC and CaMKII, decode the kinetics or temporal

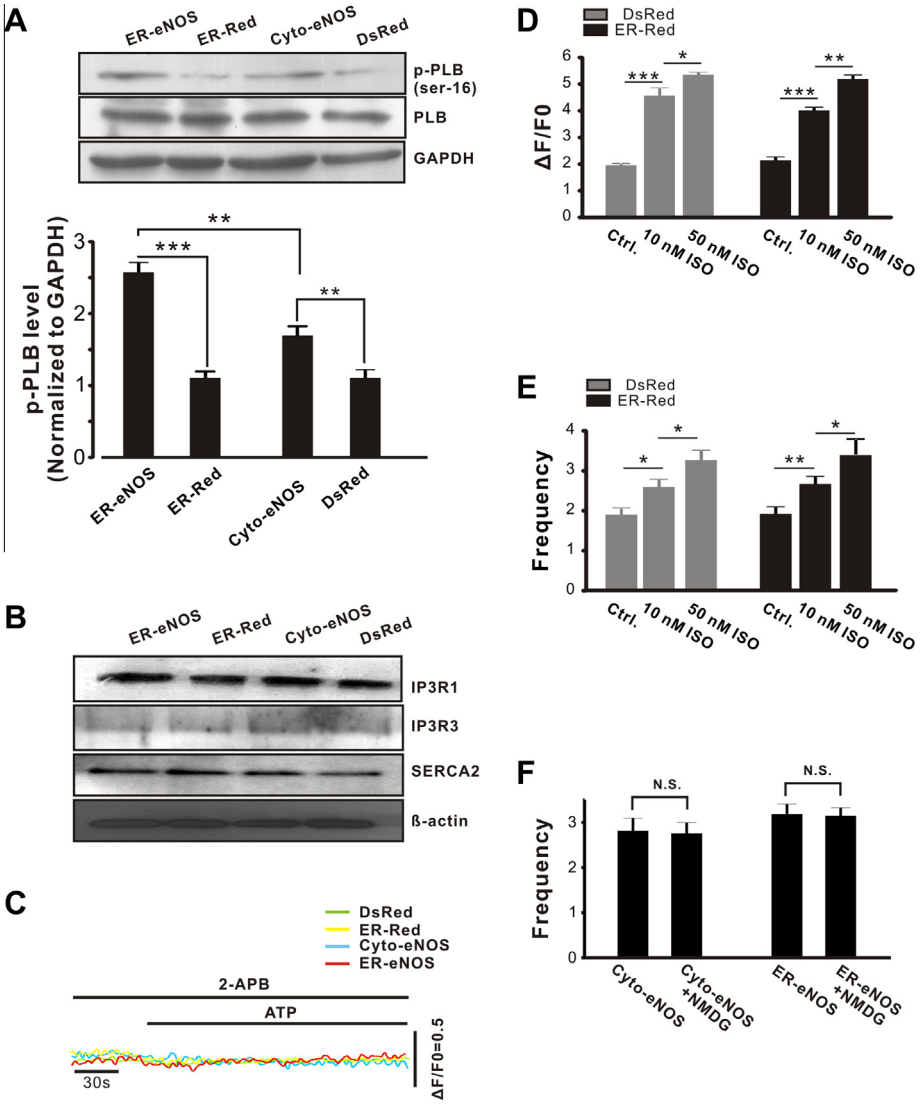

Fig. 3. eNOS overexpression up-regulates PLB (Ser-16) phosphorylation. (A) Western bolt analysis of phosphorylated PLB (Ser-16), total protein levels of PLB and housekeeping protein of GAPDH in the four types of cells (upper panel). Western blots quantified by densitometry show that PLB (Ser-16) phosphorylation (normalized to total PLB level) is significant higher in ER-eNOS than in Cyto-eNOS transfected HeLa cells (lower panel). (B) eNOS overexpression does not alter the expression of IP_3R1, IP_3R3, and SERCA2. (C) Representative profiles of Ca^{2+} fluorescence monitored by confocal imaging after 10 μM ATP application when cells were incubated with 2-APB. (D and E) In the presence of 10 nM ISO, eATP (10 μM) induced calcium signals were significantly enhanced. The amplitude ($\Delta F/F0$) (D) and frequency (E) of Ca^{2+} oscillation was increased both in DsRed cells and ER-Red cells. When the concentration of ISO was increased to 50 nM, Ca^{2+} oscillation was enhanced further ($n = 50$ from 4 independent experiments). (F) The frequency of Ca^{2+} oscillations in the eNOS overexpressing cells is not altered when NCX is blocked by NMDG ($n = 20–30$ from 3 independent experiments). All experiments were repeated at least three times. $^{*}P < 0.05$, $^{**}P < 0.01$ and $^{***}P < 0.0001$ by two-tailed Student's test.

properties of the Ca^{2+} signal and translate them into distinct cellular response [1]. The enhanced Ca^{2+} oscillation may be decoded by Ca^{2+} sensors and drive the cells to make different choices [26]. Thus, we proposed a potential way of alteration in the eNOS activity to influence the cell fate via Ca^{2+} oscillation. However, some processes of cellular activities, like proliferation, migration and more specific downstream targets of Ca^{2+} oscillation need to be explored in further studies.

Since there is no ryanodine receptors (RYRs) expression in HeLa cells [27,28], we believe that the enhanced Ca^{2+} oscillation induced by NO is mediated by IP3 receptors. There are three isoforms of IP_3R, namely IP_3R1, IP_3R2, IP_3R3, with different tissue distribution. Type 1 and type 3 IP_3R have been thought to be important for the generation of Ca^{2+} oscillations in HeLa cells [27], which was mainly attributed to the calcium release form intracellular stores but not extracellular matrix [29]. However, we found that IP_3R1 and IP_3R3 expression was not altered in the eNOS overexpressing cells (Fig. 3B). Enhanced Ca^{2+} re-uptake efficiency indicates that overactive SERCA is involved in the modulation of Ca^{2+} oscillation. Despite SERCA2 expression level was not changed, the phosphorylation level of PLB (Ser-16) was greatly up-regulated in the eNOS overexpressing cells (Fig. 3A), which suggests that the inhibitory status of SERCA is partly removed and this is mediated by NO-cGMP-PKG pathway considering that the serine 16 site of PLB is phosphorylated by PKG or PKA [19,20]. Overactive SERCA facilitates Ca^{2+} re-uptake during the IP3 induced Ca^{2+} release followed by the increase in the frequency and amplitude of Ca^{2+} oscillation. On the contrary, inhibition of SERCA totally diminished the eATP induced Ca^{2+} oscillation (Fig. 4A). Previous study showed that increase in the SERCA activity by removing the influence of PLB leads to the increase of ER Ca^{2+} load in the diabetic heart [30]. Consistently, we found that ER Ca^{2+} load was much higher in the eNOS

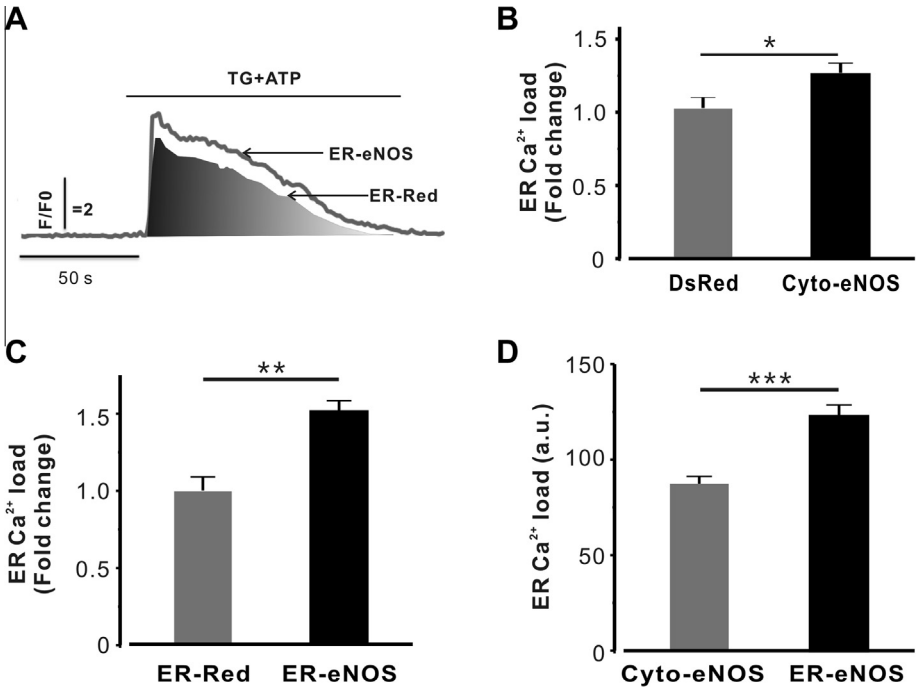

Fig. 4. eNOS overexpression increases ER Ca^{2+} load. (A) Representative profiles of Ca^{2+} transients induced by 100 μM ATP in the presence of TG in ER-eNOS and ER-Red transfected HeLa cells. The integration of the normalized fluorescence intensity to time was calculated as the ER calcium load (gray area) in ER-Red transfected cells. (B) & (C) Summary data of ER Ca^{2+} load in Cyto-eNOS (B) and ER-eNOS (C) overexpressing cells, respectively. The ER Ca^{2+} load of ER-eNOS and Cyto-eNOS overexpressing cells was normalized to their controls, respectively. (D) Comparison of ER Ca^{2+} load between the ER-eNOS and Cyto-eNOS overexpressing cells, the values of ER Ca^{2+} load were calculated as the integration of fluorescence intensity to time in Origin 8 (n = 20–30 cells from 5 independent experiments). $^{*}P < 0.05$, $^{**}P < 0.01$ and $^{***}P < 0.0001$ by two-tailed Student's test.

overexpressing cells, which further explains the enhancement of Ca^{2+} oscillation in those cells. Furthermore, we noted that the ER-eNOS cells displayed much higher amplitude of Ca^{2+} oscillation and ER Ca^{2+} load compared to the Cyto-eNOS cells. This could be partly interpreted by the different spatial distance between SERCA and eNOS in the two types of cells. Although NO is considered as a diffusible signal molecule [31,32], the extent of the influenced area can be greatly changed by NOS location [33–35].

Conclusion

Our study reveals that overexpression of eNOS in Cytosol and ER of HeLa cells significantly alters the properties of Ca^{2+} oscillation induced by eATP, and this change of Ca^{2+} oscillation properties by eNOS overexpression is mediated by the increases in the ER Ca^{2+} load due to hyper-phosphorylation of PLB and followed by the activation of SERCA.

Acknowledgments

This work was supported by Grants from the National Basic Research Program of China (2011CB809104 to GJ) and the National Foundation of Sciences and Technology (31271228 to GJ).

Appendix A. Supplementary data

Supplementary data associated with this article can be found, in the online version, at http://dx.doi.org/10.1016/j.abb.2014.11.006.

References

[1] A.B. Parekh, Trends Biochem. Sci. 36 (2011) 78–87.
[2] H. Cheng, W.J. Lederer, Physiol. Rev. 88 (2008) 1491–1545.
[3] D.E. Clapham, Cell 131 (2007) 1047–1058.
[4] A. Sakurai, S. Oda, Y. Kuwabara, S. Miyazaki, Mol. Hum. Reprod. 5 (1999) 132–138.
[5] M. Vig, J.P. Kinet, Nat. Immunol. 10 (2009) 21–27.
[6] J.H. Shah, D.J. Maguire, D. Brown, A. Cotterill, Adv. Exp. Med. Biol. 599 (2007) 133–138.
[7] N.L. Siow, R.C. Choi, H.Q. Xie, L.W. Kong, G.K. Chu, G.K. Chan, J. Simon, E.A. Barnard, K.W. Tsim, Mol. Pharmacol. 78 (2010) 1059–1071.
[8] Z. Chen, Z. Li, G. Peng, X. Chen, W. Yin, M.I. Kotlikoff, Z.Q. Yuan, G. Ji, Biochem. Biophys. Res. Commun. 382 (2009) 381–384.
[9] P.B. Massion, O. Feron, C. Dessy, J.L. Balligand, Circ. Res. 93 (2003) 388–398.
[10] I. Fleming, R. Busse, Cardiovasc. Res. 43 (1999) 532–541.
[11] B. Wei, Z. Chen, X. Zhang, M. Feldman, X.Z. Dong, R. Doran, B.L. Zhao, W.X. Yin, M.I. Kotlikoff, G. Ji, PLoS ONE 3 (2008) e2526.
[12] C. Pott, D. Steinritz, B. Bolck, U. Mehlhorn, K. Brixius, R.H. Schwinger, W. Bloch, Am. J. Physiol. Cell Physiol. 290 (2006) C1437–C1445.
[13] J.K. Bendall, T. Damy, P. Ratajczak, X. Loyer, V. Monceau, I. Marty, P. Milliez, E. Robidel, F. Marotte, J.L. Samuel, C. Heymes, Circulation 110 (2004) 2368–2375.
[14] B. Wei, W. Dui, D. Liu, Y. Xing, Z. Yuan, G. Ji, BMC Biol. 11 (2013) 12.
[15] W. Dui, B. Wei, F. He, W. Lu, C. Li, X. Liang, J. Ma, R. Jiao, Mol. Biol. Cell 24 (1676–1687) (2013) S1671–S1677.
[16] H. Kojima, Y. Urano, K. Kikuchi, T. Higuchi, Y. Hirata, T. Nagano, Angew. Chem. 38 (1999) 3209–3212.
[17] Y. Zhu, H.L. Liao, X.L. Niu, Y. Yuan, T. Lin, L. Verna, M.B. Stemerman, Biochim. Biophys. Acta 1635 (2003) 117–126.
[18] C. Ruiz-Holst, B. Bolck, A. Ghanem, K. Tiemann, S. Brokat, V. Regitz-Zagrosek, W. Bloch, R.H. Schwinger, K. Brixius, Can. J. Physiol. Pharmacol. 88 (2010) 121–129.
[19] J. Colyer, Ann. N.Y. Acad. Sci. 853 (1998) 79–91.
[20] T.M. Lincoln, N. Dey, H. Sellak, J. Appl. Physiol. 91 (2001) 1421–1430.
[21] R. DiPolo, L. Beauge, Physiol. Rev. 86 (2006) 155–203.
[22] A.K. Cardozo, F. Ortis, J. Storling, Y.M. Feng, J. Rasschaert, M. Tonnesen, F. Van Eylen, T. Mandrup-Poulsen, A. Herchuelz, D.L. Eizirik, Diabetes 54 (2005) 452–461.
[23] S. Wenzel, C. Rohde, S. Wingerning, J. Roth, G. Kojda, K.D. Schluter, Hypertension 49 (2007) 193–200.
[24] C. Bogdan, Nat. Immunol. 2 (2001) 907–916.
[25] C. Xu, B. Bailly-Maitre, J.C. Reed, J. Clin. Invest. 115 (2005) 2656–2664.
[26] M. Colella, F. Grisan, V. Robert, J.D. Turner, A.P. Thomas, T. Pozzan, Proc. Natl. Acad. Sci. U.S.A. 105 (2008) 2859–2864.
[27] M. Hattori, A.Z. Suzuki, T. Higo, H. Miyauchi, T. Michikawa, T. Nakamura, T. Inoue, K. Mikoshiba, J. Biol. Chem. 279 (2004) (1975) 11967–11975.
[28] T. Higo, M. Hattori, T. Nakamura, T. Natsume, T. Michikawa, K. Mikoshiba, Cell 120 (2005) 85–98.
[29] L. Welter-Stahl, C.M. da Silva, J. Schachter, P.M. Persechini, H.S. Souza, D.M. Ojcius, R. Coutinho-Silva, Biochim. Biophys. Acta 1788 (2009) 1176–1187.

[30] D.D. Belke, W.H. Dillmann, Curr. Hypertens. Rep. 6 (2004) 424–429.
[31] F. Schreiber, L. Polerecky, D. de Beer, Anal. Chem. 80 (2008) 1152–1158.
[32] S.R. Ott, A. Philippides, M.R. Elphick, M. O'Shea, Eur. J. Neurosci. 25 (2007) 181–190.
[33] Y. Yang, G.M. Ning, J. Kutor, D.H. Hong, M. Zhang, X.X. Zheng, Cell Biol. Int. 28 (2004) 577–583.
[34] J.M. Hare, Lancet 363 (2004) 1338–1339.
[35] L.A. Barouch, R.W. Harrison, M.W. Skaf, G.O. Rosas, T.P. Cappola, Z.A. Kobeissi, I.A. Hobai, C.A. Lemmon, A.L. Burnett, B. O'Rourke, E.R. Rodriguez, P.L. Huang, J.A. Lima, D.E. Berkowitz, J.M. Hare, Nature 416 (2002) 337–339.